

# Continuous drive dissimilar friction welding of wrought aluminium AA6063-T6 and austenitic stainless steel AISI304L with different welding methods and welding trials

S. Senthil Murugan\*, P. Sathiya, A. Noorul Haq

*Department of Production Engineering, National Institute of Technology (NIT),  
Tiruchirappalli 620 015, Tamilnadu, India*

Received 9 March 2021, received in revised form 21 May 2021, accepted 03 June 2021

## Abstract

Welding dissimilar metals by fusion welding process is a tough task, as both metals have different thermomechanical properties. In this study, experiments are carried out to join aluminium AA6063-T6 and steel AISI304L dissimilar alloys with different faying surface modifications through a continuous drive friction welding process (CDFW). This study aims to introduce the joining methods and evaluate the performance of their fabricated joints through microstructure and mechanical characterisations. Here, friction time (3, 5, and 7 s) is varied, whereas friction and upset pressures are kept constant. The faying surface-modified specimens are welded at constant chuck rotational speed 1300 rpm. The surface of the AISI304L specimen is buttered with pure aluminium and welded with an AA6063-T6 specimen. Similarly, the faying surface of the AISI304L specimen is tapered and welds with AA6063-T6 specimens having different modifications like a flat, tapered, and internal groove on their faying surfaces. Thus, different welding trials with different friction timings are conducted for each modification. The results of such joining methods like axial shortening, microstructures, EDS spectrums, tensile properties, impact strength, fractography, and Vickers microhardness are discussed and compared in this paper. The surface modifications with friction time improved the strength and 108.8 % joint efficiency.

**Key words:** faying surface, dissimilar joint, AA6063-T6, mechanical properties, AISI304L, friction welding, joint efficiency

## 1. Introduction

In the manufacturing industries, similar joints have often been substituted with dissimilar joints that may have a comparatively high strength-to-weight ratio. However, the welding of such dissimilar joints requires sophisticated processes and must be done under high scrutiny. Welding of ferrous metal with non-ferrous metal is quite challenging due to the varied physical and chemical properties of the metals [1]. The conventional problems related to welding dissimilar joints can be overcome by solid-state welding [2]. The utilisation of advanced welding techniques to join dissimilar metals is needed as the conventional welding processes are ineffective. Joining dissimilar metals is possible by friction welding (FW) process with outstanding weld

quality, which is also economical [3–5]. FW is an eco-friendly and solid-state joining process that causes no melting of parent materials that means the welding temperature is lesser than the melting temperature of the base metals. Inertia friction welding (IFW) can also be used instead of CDFW as the drive required is small for similar specimen dimensions. It is also a proven weld technique with a regression model to test the influence of parameters [5].

The concept of friction welding shown in Fig. 1 was followed in this study. The non-rotating specimen is kept at the right-side holder activated by a hydraulic ram in the friction welding machine. The specimen kept at the chuck creates rotary motion due to the spindle rotation in the machine, and the other part produces an axial movement with pressure called fric-

\*Corresponding author: e-mail address: [gctsegan@gmail.com](mailto:gctsegan@gmail.com)

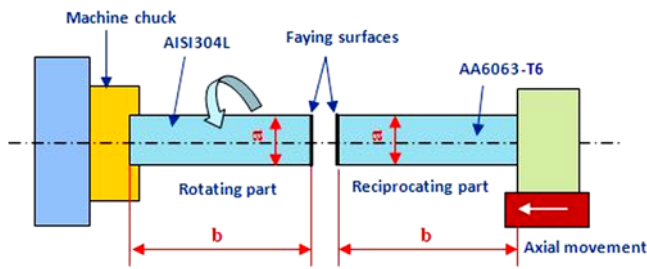


Fig. 1. Rotary friction welding followed in this study ( $a = \varnothing 12 \text{ mm}$ ,  $b = 100 \text{ mm}$ ).

tion pressure (FP) to raise interface temperature to a plastic state by frictional effect with the material at chuck over a period of time called friction time (FT) or heating time. Finally, an additional pressure (upset pressure – UP) is applied for some time on the weld joint when friction is stopped to complete the weld [6]. In FW, the coalescence is obtained by the synergic effect of pressure and the relative motion between the parts to be welded over a while. Iracheta et al. [7] used IFW to weld CrMoV based steel and developed a finite element model to predict the residual stress during the IFW. The significant problems to be considered during friction welding include the formation of brittle intermetallics, the weld interface temperature, and the width of the heat-affected zone (HAZ).

Kimura et al. [8] had worked on the joining of both pure aluminium and AISI304L and evaluated the tensile strength and the bend ductility of the joint. The weld interface temperature reached a maximum with an increase in FT. The maximum temperature on the weld interface was about  $300^\circ\text{C}$  at 2 s friction time during FW. The main intermetallics developed when joining aluminium and stainless steel dissimilar alloys are FeAl (Fe rich),  $\text{FeAl}_2$ ,  $\text{Fe}_3\text{Al}$ ,  $\text{FeAl}_{16}$ ,  $\text{Fe}_2\text{Al}_5$  (Al rich),  $\text{Fe}_2\text{Al}_3$ , and  $\text{FeAl}_3$ . These intermetallics may weaken the weld strength; thus, it is necessary to choose the welding technique suitable for improving the weld quality by reducing the intermetallic formation and narrowing the HAZ. In conventional welding, materials are prone to participating in the reaction at elevated welding temperature [9]. The authors researched welding TC-17 titanium alloy by linear friction welding (LFW) and measured the internal residual stress distribution using the contour method.

However, FW has the significance of producing sound joint (dissimilar/similar) with narrow HAZ, thermomechanically affected zone (TMAZ) and minor intermetallics at low interface temperature. Meisnar et al. [10] proved that the possibility of joining dissimilar friction welding with no intermetallic compounds (IMC) and having the grain refinement and elongation in the vicinity of weld interface when did research on joining AA6082 and Ti-6Al-4V for aerospace applications. The study showed the possibility of resid-

ual stress in solid-state welding as well. Buffa et al. [11] used the LFW process for joining the aluminium 2011-T3 alloy to identify the temperature-dependent friction coefficient and shear stress acting on the weld zone. This research is used to understand the bonding mechanism of the LFW process.

Akram et al. [12] welded dissimilar metals P21 and AISI304 through continuous drive friction welding and analysed the creep behaviour of the joints. Their work implied that a transgranular fracture mode was observed, and the damage was mainly due to the cavity growth. In IFW, the ‘UP’ is to be kept as low as possible, without compromising the weld quality, to tolerate the torsional loading of the IFW machine. High forge pressure is recommended for a good joint. During FW, temperature and stress developed are governing welding parameters, so a piece of knowledge is needed to identify the optimum parameters, thus improving the design of joining dissimilar metals. The literature showed that the finite element method can also be used to predict the microstructure, temperature distribution and to model a joint with high quality [3, 13]. Supriya et al. [14] researched AA6063 alloy to predict the yield strength through the classical model and Orowan model. Their research concluded that the Orowan model is better to predict the yield strength, and the results are helpful to develop maps for thermal processing to attain a needed level of yield strength for AA6063-T6 alloy for the joining.

The butt-dissimilar weld of mild steel and aluminium alloy plates could be possible by friction stir welding process [15], and the effect of oxide film on the faying surface of steel was investigated. The weld efficiency was about 86 %, and the intermetallics were confirmed at the interface. As a result of the rubbing action during the welding, the oxide film was removed from the faying surfaces. Hee-Seon Bang et al. [16] joined the dissimilar alloys AA5052 aluminium & SPFCDP590 steel through friction stir welding and achieved a maximum tensile strength of 178 MPa.

This paper focuses on joining AA6063-T6 and AISI304L dissimilar alloys with different welding/joining methods (A–E) at different welding trials, and comparing their axial shortening and mechanical properties of the friction-weld joints. The welding methods are differentiated based on the faying surface modifications on the weld specimens. Faying surface means the area where the physical contact takes place on the two parts during friction welding. However, the works related to faying surface modifications were not found in literature, many works for dissimilar joining on the combinations of different alloys like pure aluminium and AISI304L [8], AA6082 and Ti-6Al-4V [10], AISI304L and alloy steel [12], AISI1018 steel and AA6061-T6 aluminium [17], AA6061-T6 and AISI4340 [18], AA6061-T6 aluminium matrix composite and AISI304 [19], and titanium and AISI304 [20],

Table 1. Chemical composition of base metals (wt.%)

Material: AISI304L									
Elements	Cr	Ni	Mn	Si	P	C	S	Fe	
	19.15	8.09	1.43	0.38	0.034	0.023	0.009	Balance	
Material: AA6063-T6									
Elements	Al	Si	Mg	Fe	Zn	Mn	Cu	Ti	Cr
	98.58	0.50	0.41	0.26	0.061	0.044	0.029	0.02	0.009

etc. were witnessed through the literature survey, but the research for the dissimilar joining of AA6063-T6 and AISI304L alloys with CDFW is still limited with the minimum required welding pressures.

To the best of knowledge, no such solid-state welding method was tried before joining steel AISI304L and aluminium AA6063-T6 rods with 100 mm length and 12 mm diameter with the welding parameters chosen in this paper. The selection of the materials was based on their different properties, such as melting point and their usage in various sectors. This new approach is initiated for the benefit of researchers around the world. From the application point of view, both materials are commercially used by industries. Through this investigation, the effects of the faying surface modifications and the welding parameters on the microstructure and the mechanical properties of the dissimilar joints are understood.

## 2. Materials and methods

### 2.1. Materials

The materials AA6063-T6 (Non-ferrous aluminium alloy) and AISI304L (Ferrous austenitic stainless steel with low carbon content) were chosen for the study since they are widely used in our home appliances and industries. The elements present in the base materials were confirmed by the optical emission spectroscopy (OES) as per ASTM E1251 standard. The chemical compositions of the materials obtained through OES are presented in Table 1, and their properties are in Table 2. Both alloys have different properties due to their different compositions. AISI304L has excellent corrosion resistance in aerospace, household activities, power plant, and automobile industries. It contains a maximum of 0.023 % carbon which is low in quantity and designated with the letter ‘L’. It has major elements of around 19 % Cr followed by 8 % Ni.

Fusion welding is not recommended for AISI304L metal as it releases hexavalent chromium Cr (VI). AA6063-T6 is a medium-strength architectural alloy with a low melting temperature (around 650 °C)

Table 2. Properties of AISI304L and AA6063-T6 (at room temperature)

Properties	AISI304L	AA6063-T6
Melting point (°C)	1450	616-654
Young’s modulus (GPa)	193	68.9
Vickers hardness, HV	200	80
Elongation (%) (min.)	45	10
Tensile strength (MPa)	515	205
Density (g cm <sup>-3</sup> )	8.0	2.7

compared to AISI304L [21]. In AA6063-T6, silicon presents only 0.5 %, followed by magnesium (0.41 %) and iron element (0.26 %), and it is quite popular in applications [22] like architectural fabrication, window and doors, cycle frames, furniture, pipe and tubing since it is lightweight and has good properties, good machinability, heat treatable, and weldable metal.

### 2.2. Methods

In this study, different welding trials with different welding methods were carried out to join AISI304L, and AA6063-T6 tempered dissimilar alloys through the CDFW following the concept shown in Fig. 1. Figure 2 shows the five different welding methods (A–E) of this study. Here, the AISI304L alloy was rotating at the chuck of the KUKA friction welding machine, and the AA6063-T6 alloy was axially reciprocating against the rotating alloy. The welding trials were fixed based on the welding methods and the friction time 3, 5, and 7 s, as given in Table 3. Initially, the welding specimens (Figs. 3a–f) of 100 mm length and 12 mm diameter were prepared for the experiments to be done by the methods ‘A’ to ‘E’.

The welding method ‘A’ (welding trials A1–A3) means the friction welding was done between the AISI304L & AA6063-T6 specimens, in which the faying surfaces are flat, as shown in Fig. 2. The method ‘B’ (as in Fig. 2) means that the joints were fabricated between the AA6063-T6 specimen having a flat

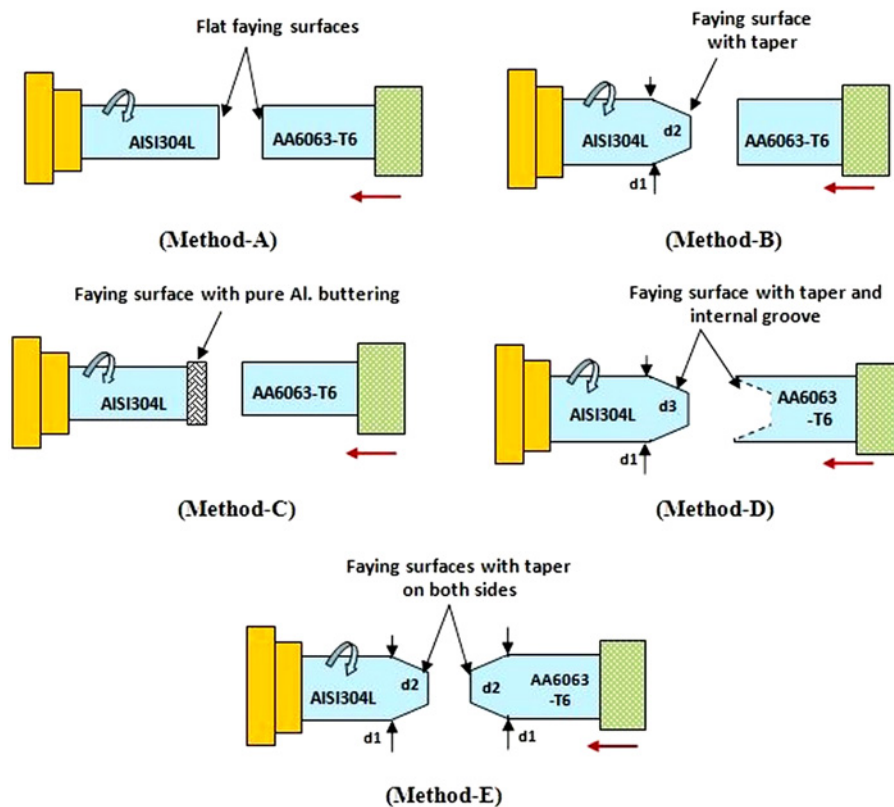


Fig. 2. Friction welding methods (A–E) with different faying surfaces tried in this study, (where  $d_1 = \varnothing 12$  mm,  $d_2 = \varnothing 9$  mm,  $d_3 = \varnothing 6$  mm).

Table 3. Experimental parameters for the welding methods (A–E) and trials for this study

Experiments	FT (s)	Welding pressures (MPa)
Welding trials: A1, B1, C1, D1, E1	3	FP = 18, UP = 24, are constant for all welding trials (A1–E3)
Welding trials: A2, B2, C2, D2, E2	5	
Welding trials: A3, B3, C3, D2, E3	7	

surface and the surface tapered AISI304L specimen. The method ‘C’ (Fig. 2) is meant for the welding between the AISI304L specimen, in which faying surface was modified by the buttering [23] of pure aluminium made by dipping process and the AA6063-T6 specimen, which has a flat surface. The method ‘D’ (Fig. 2) is meant for the welding between the AISI304L specimen with tapering and the AA6063-T6 specimen with an internal groove. But the method ‘E’ (Fig. 2) is meant for the joining between the faying surfaces tapered AISI304L and AA6063-T6 specimens.

However, the FP, UP, upset time, rotational speed, and axial penetration were constantly maintained as 18 and 24 MPa, 3 s, 1300 rpm, and  $3 \text{ mm s}^{-1}$ , respectively, throughout all experiments. Friction time, upset time, burn-off length and speed are the parameters controlling the friction welding efficiency. For instance, the creation of FeAl<sub>3</sub> brittle IMC may be controlled by

increasing the speed [24, 25]. Kimura et al. [8] identified that the weld interface becomes thicker if the heating time increases. AA6063 has a soft and medium strength, so less FP may be enough for solid-state joining. AISI304L is averagely hard, so moderate FP is needed to get effective bonding with aluminium alloys [26]. Unfortunately, the joints fabricated with huge FP showed maximum axial shortening and crush, cracks and the joints got damaged due to the overload. If the UP is recommended to be higher than the FP, it is favourable for achieving a good joint.

One of the welded joints fabricated by trial ‘B2’ is shown in Fig. 3g, where the weld flash was formed at the aluminium side. FP and UP were responsible for causing ring shape flash formation. The axial shortenings [27, 28] of the welds, which were due to the mechanical forces, were observed during the welding. Figure 3h shows the welded specimen after machin-

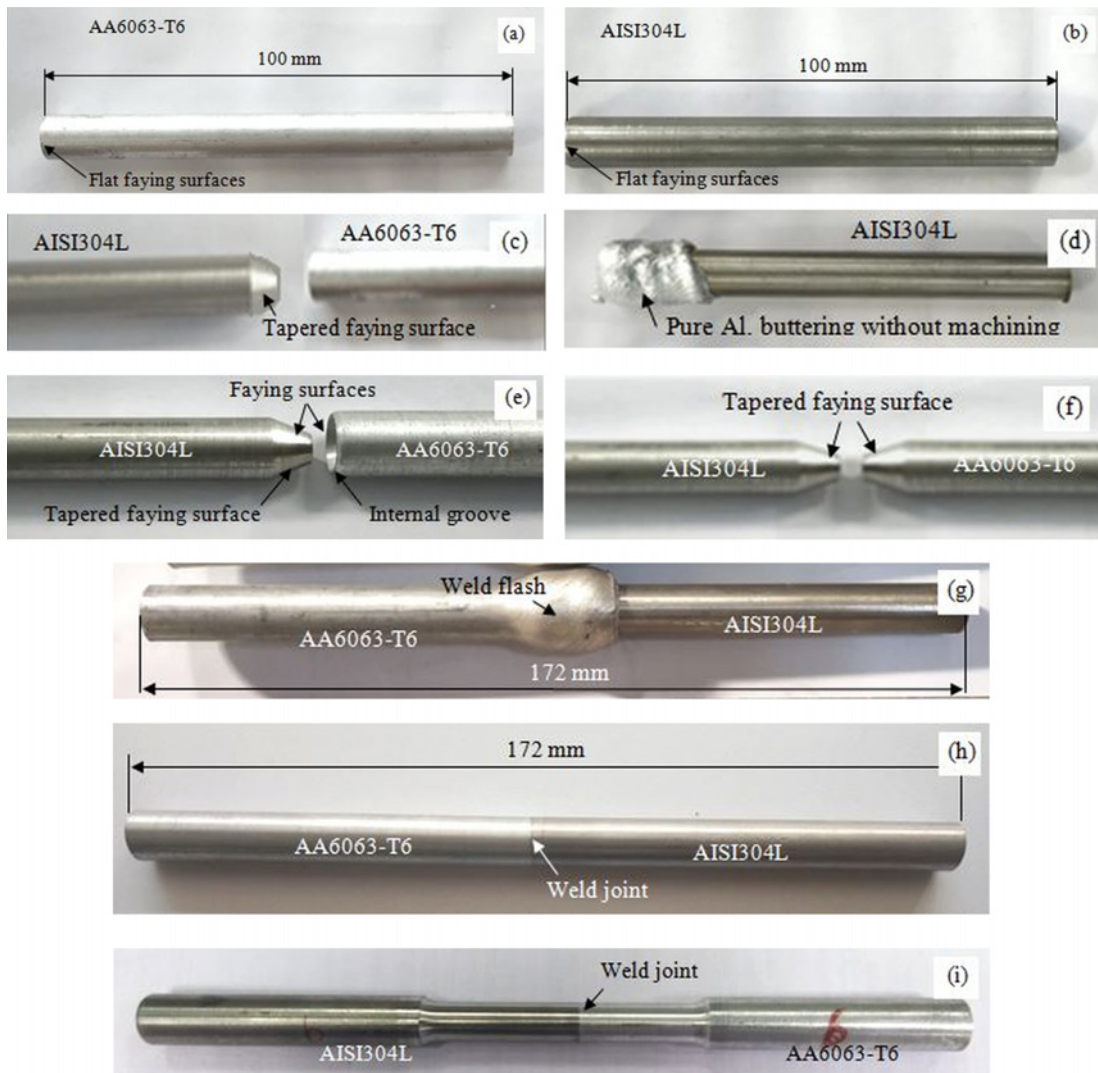


Fig. 3. Images of the weld samples and as mentioned in Figs. 1, 2, where (a) & (b) weld specimens of  $\phi$  12 mm for welding method A, (c) for method B, (d) buttered AISI304L for method C, (e) for method D, (f) for method E, and (g) dissimilar weld joint with flash prepared by 'B2' weld trial (h) weld of trial B2 after flash removal, and (i) tensile specimen of trial B2 as per ASTM E8 standard.

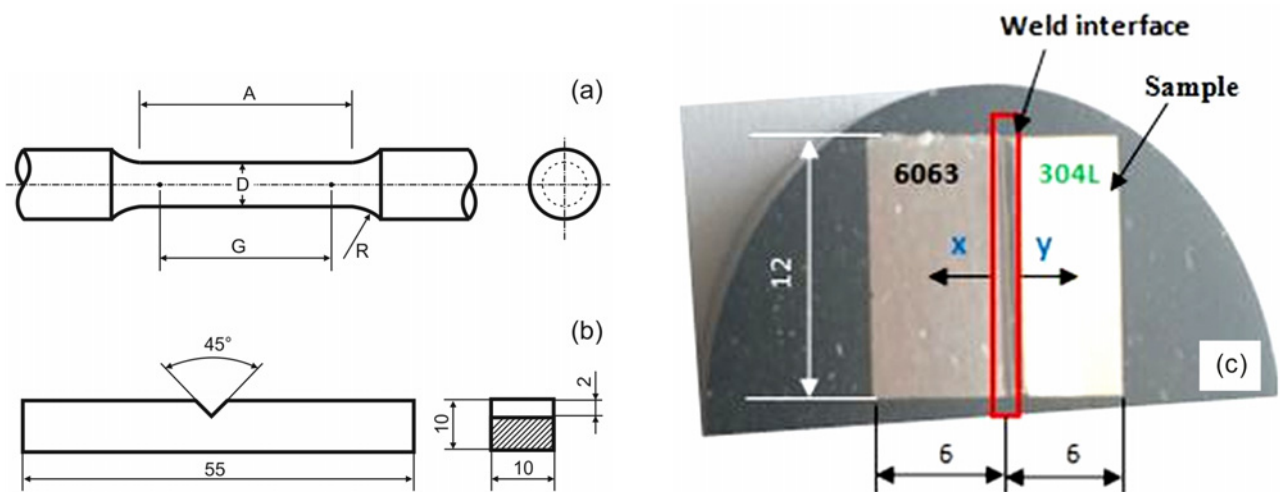


Fig. 4. Test specimens dimensions (in 'mm') for (a) tensile test where, D-9 dia., G-45, A-54, R-8, (b) V-notch impact test, and (c) microhardness measurement at  $x$ ,  $y$ -directions towards base metal from weld interface.

ing the weld flash, and Fig. 3i is the tensile sample prepared for testing as per ASTM E8 standard. For the microstructure and fracture characteristics of tensile and impact tested specimens, a scanning electron microscope (SEM) was used, and the phases and compositions present in the weld interface (WI) were identified through energy dispersive spectroscopy (EDS).

INNOVATEST Vickers hardness tester was used to determine the microhardness in the weld zone with 15 s dwell time & 0.3 kg load. The ASTM E8 standard is shown in Fig. 4a, and test specimens are tested by the MTS INSIGHT-1000 kN UTM machine. For the impact toughness testing, the samples were prepared per the ASTM E23 standard (Fig. 4b). The V-notch was positioned at the weld interface of the joints, and the testing was carried out by the MTS (SANZ)–ZBC2452 machine (maximum capability of 450 kJ impacting energy) at room temperature. Similarly, Fig. 4c shows the image of the test specimen prepared from the dissimilar joints for the microstructure and microhardness analysis. The  $x$  and  $y$  directions at which the hardness was measured on the specimen are also shown in the figure.

### 3. Results and discussion

#### 3.1. Axial shortening

In friction welding, axial shortening is the shortage in the length of the prepared joints. It was measured in the experiments by considering both the length of weld specimens (Figs. 3a–f) before the welding process and the length of the welded joints after the friction welding process. For instance, the axial shortening of trial B2 is discussed in Figs. 3a,b – before FW and Fig. 3g – after FW, where the axial shortening was recorded as 28 mm. When analysing the shortening/material loss of all the welding trials after the FW, it had to be observed that the axial shortening was in the range of 16–30 mm. The modifications with the tapering reduced the length of the weld after the experiment and increased the axial shortening. It means that the metal was consumed due to the frictional and reciprocating effect of the machine at various welding parameters.

Generally, the material loss may be varied according to the selection of parameters, geometry shape of the weld specimens and the specimen materials like ferrous or non-ferrous. But through this investigation, it has to be proved that the different faying surfaces on the weld specimens can produce different shortening for the same category of welding materials. The bar chart shown in Fig. 5 is the axial shortening of the different welding trials tried during the friction welding experiment. The method ‘C’ reported the minimum shortening because of its buttering layer of pure aluminium formed over the AISI304L alloy during FW.

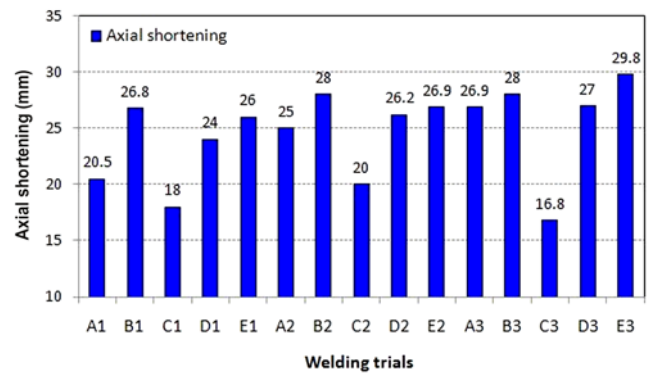


Fig. 5. Axial shortening values for the different welding trials.

From the results, it has to be accepted the effect of friction time variation and the faying surface modifications.

For instance, though the friction time for the trials A1–E1 was the same, the shortening was different because of their different faying surfaces on the weld specimen. Similarly, though the faying surface for the welding trials ‘A1–A3’ was the same, the shortening was quite varying due to its different FT during FW. In some cases, the tensile strength of the joint could be obtained high even though the shortening was more. The tapering faying surface increased the penetration of AISI304L onto AA6063-T6 alloy, reducing the weld length. This was identified for the methods B, D, and E, which have good strength with maximum shortening. This is because of the action of faying surfaces, according to their FT.

#### 3.2. Microstructure and EDS analysis

The welded joints were studied through microstructures and EDS analysis. The EDS was helpful to understand the elements formed at the WI. The SEM images available in Figs. 6a–e show the weld zones of weld joints prepared through the welding methods A to E, respectively. Here, the microstructure and EDS were characterised for the joints with maximum tensile strength for the different trials. Figure 6a shows the weld zone of joining method ‘A’. The bonding between AA6063-T6 alloy and AISI304L alloy was quite good by the method ‘A’, and a narrow WI was observed from the SEM image. Figure 6b is for the welding trial ‘B2’. Since method ‘B’ had the tapering on its AISI304L alloy side during FW, the shape of the WI was like the alphabetical letter ‘V’, as shown in Fig. 6b. This was due to the penetration of AISI304L alloy into the alloy AA6063-T6 during the axial movement of the frictional force.

While analysing the WI, it was thought that the tapering effect improved the bonding strength between

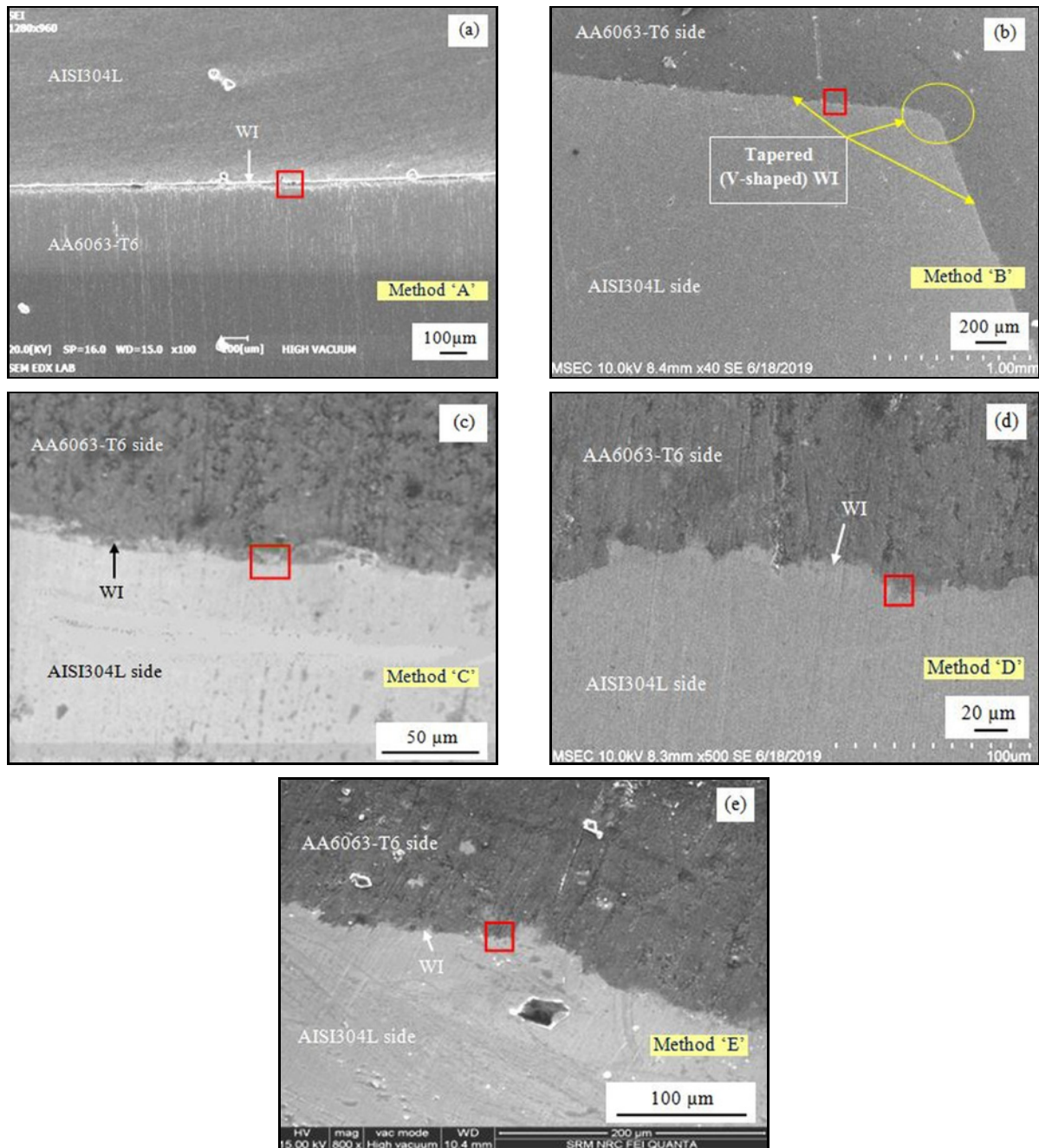
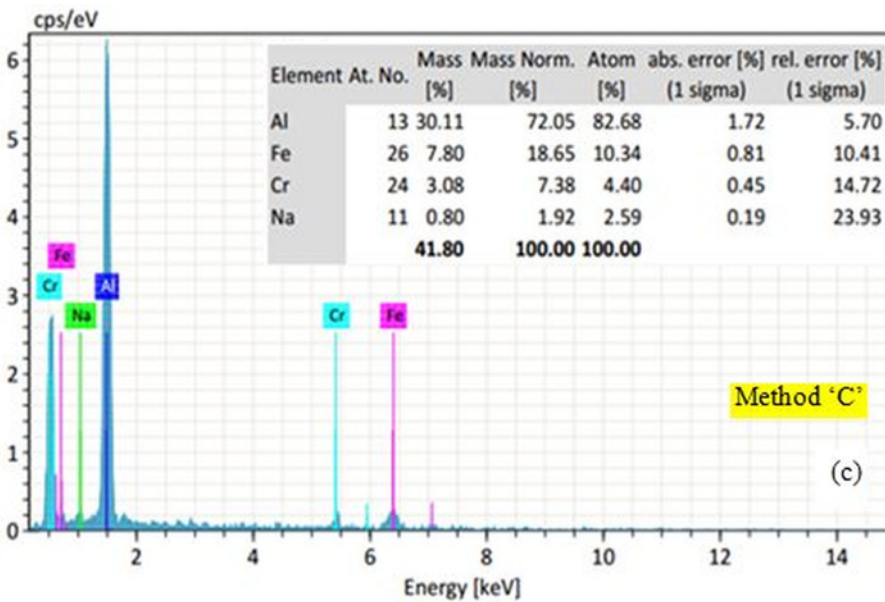
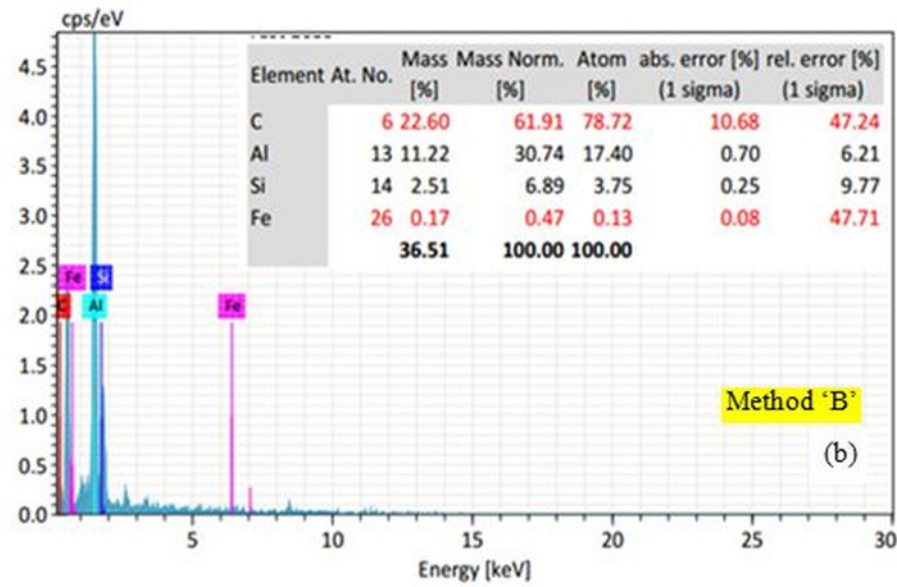
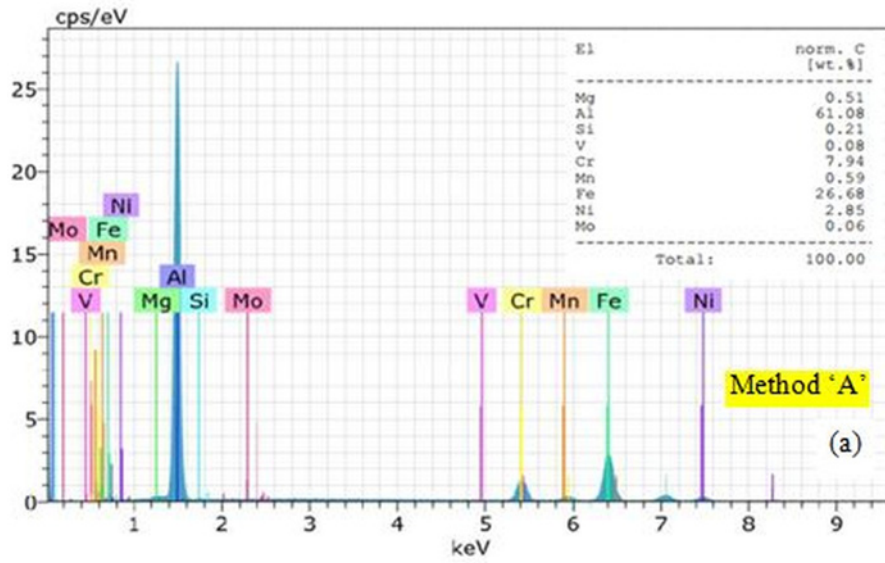


Fig. 6. SEM images of weld zone of joining methods A to E, where image (a) of trial A2, (b) of trial B2, (c) of trial C2, (d) of trial D3, and (e) of trial E2. (WI – weld interface)

the dissimilar alloys. The WI of the joint on Fig. 6c was prepared by the method 'C', which newly introduced the buttering layer of pure aluminium on the AISI304L specimen. Welding of stainless steel to aluminium can be done by using this layering technique. The pure aluminium layer was completely defused during the FW at high frictional force and speed. The purpose of this technique was to reduce the weak intermetallics at the weld interface. The bonding was good and smooth between AA6063-T6 and AISI304L, but not much strength was recorded. This was mainly

due to the improper welding parameter. It was also noted that if the buttering concept is used, it may need much more high welding parameters like speed, friction time, and friction pressure. Also, the surface finish of the buttering on AISI304L is important, which may affect the joining phenomenon. Figure 6d is the weld interface of the joining method 'D' and trial D3. The bonding was good and robust and, in turn, increased its tensile strength.

The internal groove (deep recess) available on the AA6063-T6 side perfectly accommodated the tapering



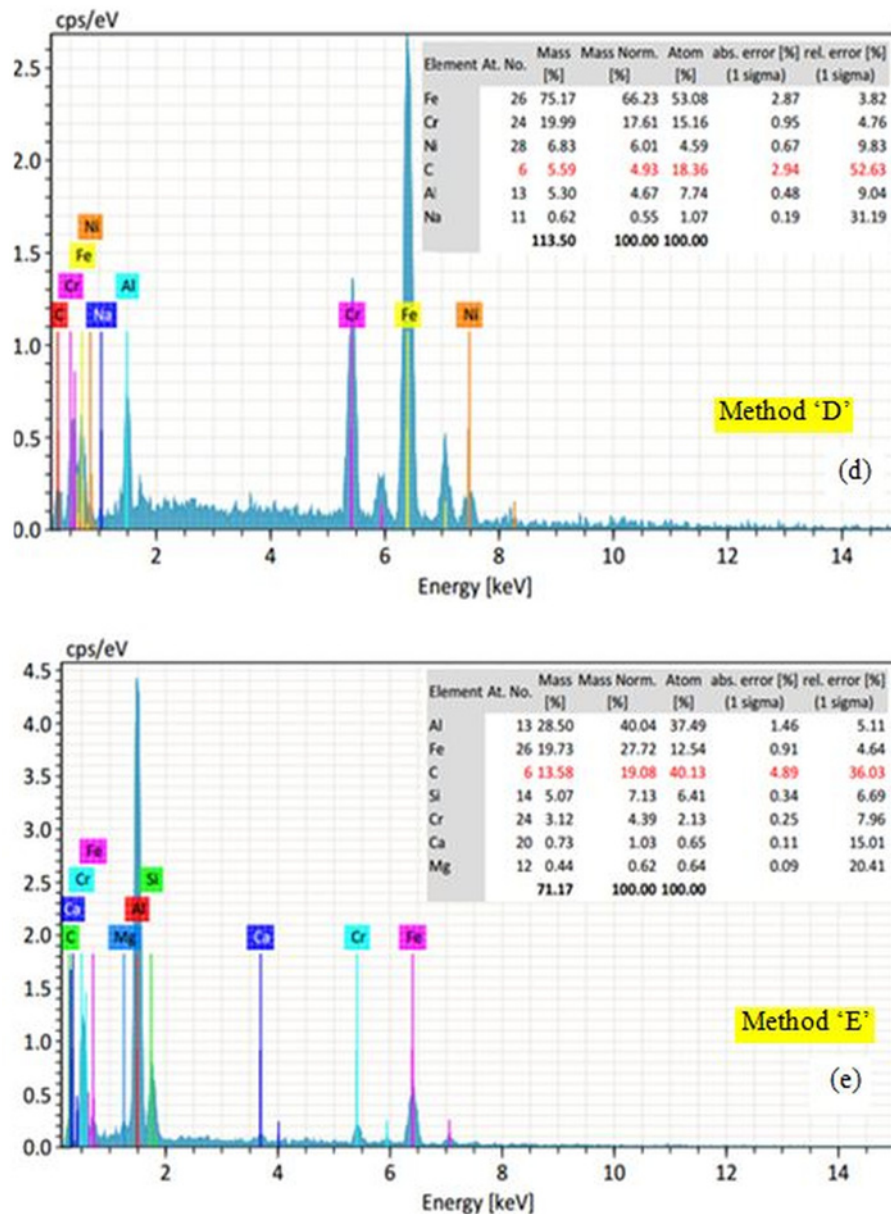


Fig. 7. EDS spectra on weld interface of friction welded joints, where spectrum (a) of trial A2, (b) of trial B2, (c) of trial C2, (d) of trial D3, (e) of trial E2.

of the AISI304L specimen during FW. The penetration by the AISI304L alloy onto the AA6063-T6 alloys is visible in the image. This method was used for increasing the bonding strength between the dissimilar joint. The HAZ of both AA6063-T6 and AISI304L side shows deformed grains. This method required more FT for excellent strength. The weld joint of the trial E2 is shown in Fig. 6e. The joint produced was strong and smooth. The WI was not in a straight line but was in a concave manner. The AA6063-T6 debris, because of the frictional effect, was shown on the AA6063-T6 side. It needs a slightly higher FP for good strength.

In this study, EDS analysis was used to identify the elements present in the welded joints (weld in-

terface). This study showed the formation of Fe-Al intermetallics. The EDS spectra of the weld interface (Figs. 6a–e) prepared by the individual welding method are given in Figs. 7a–e. The joints by the welding trials, which gave the maximum tensile strength, were used for this study. Figure 7a shows the point EDS spectrum of welding trial A2 since it gave maximum tensile strength among the other trials in method A. The WI (Fig. 6a) contains Fe and Al as maximum, followed by Cr, Ni, etc. The elements Mg, Si, V, and Mo were also found at a trace level. The formation of 'Mo' improves the joint property, and the element 'Si' improves the hardness.

From Fig. 7b, the EDS of trial B2 is read. It proved

the elements like Fe, C, Al, and Si present at the WI. However, the interface of joining trial 'C2' (Fig. 7c) had Al, Fe, Cr, and Na. The content of aluminium was huge, which was about 72 %. So, the formed intermetallics can have poor strength. Similarly, the EDS spectrum (Fig. 7d) of weld trial 'D3' at the weld joint showed the elements like Fe, Cr, Al, and Na, etc., as the D3 trial had maximum strength in the welding method 'D'. It produced good strength, and the bonding formed the maximum of the elements of 17.6 % Cr, which improves the corrosion property of the joint with nickel by about 6 %. The 'Na' generally improves the heat transfer capability of the metal. The joint fabricated by the welding trial D3 generated 0.6 % of Na. Figure 7e shows the Point-EDS analysis of weld produced by method E with trial E2. The joint interface contained Al, Fe, Si, Cr, C, Ca, and Mg elements. Unlike other methods and their trials, this trial produced 'Ca' at WI of the prepared dissimilar joints, which has a powerful chemical affinity for O<sub>2</sub>. The red box in Fig. 6 is the place where EDS was analysed.

### 3.3. Tensile properties and fracture analysis

The testing specimens were prepared as per the standard, and the tensile strength [29] of each weld was measured using a universal testing machine. Most of the breakage took place outside of the weld joint during the test. The results obtained through tensile testing like tensile and yield strength, axial shortening relation with weld strength, weld efficiency, peak load, % elongation, tensile-to-yield strength (TS/YS) ratio and tensile and yield strength (TS–YS) difference are reported here from Figs. 8a–g, respectively. Among the trials A1–A3 of the method 'A' with flat faying surfaces, the maximum tensile strength of the weld joint was about 189 MPa (Fig. 8a); for the trial A2 at FT 5 s, the FT changed the tensile properties of the joint. With the A1 trial, the required FT for the joining would be less, so the strong bonding between metals lacked a short duration. At the same time, welding with the 7 s FT increased the frictional heat at high pressure and was over softening the soft material AA6063-T6 and, in turn, reduced the weld strength.

The correlation between the axial shortening and the weld strength is given in (Fig. 8b); when the axial shortening increases, the tensile and yield strength increases and retains almost constant if the axial shortening is between 27–30 mm. Joint efficiency (Fig. 8c) maximum of 92 % was obtained for 5 s FT (trial A2) by the method 'A'. It can further be increased by the changes in the surface modifications and the various parameters. The peak load during the tensile testing of the joints fabricated by the method 'A' was almost equal to 12 kN (Fig. 8d), and the < 10 % elongation (Fig. 8e) was observed during the test. Thus the varia-

tion of FT can change the weld joints properties; even a minor change can cause appreciable changes in their properties. The strain hardening behaviour can be determined by TS/YS ratio (Fig. 8f). Here, it was almost 1.05 maximum. Similarly, the TS–YS value (Fig. 8g) was also less than 9 MPa. This flat faying surface is not giving the expected level of TS/YS ratio and TS–YS values.

The experiments (B1–B3 trials) with a taper on faying/welding surfaces of AISI304L showed very good results; the maximum tensile strength recorded was 219 MPa (trial B2) for 5 s FT with the weld efficiency of 107 %. It was understood that the tapering effect might reduce the FT required for the material joining and increase the strength. The maximum peak load received by the joint was about 14 kN. The % elongation for all the trial under this method was 10 % as the FT did not show the effect on the elongation property. The strain hardening ratio (TS/YS) achieved a maximum of 1.23 for trial B1. Method 'B' showed a good strain hardening rate, which is necessary for the ductility measurement, compared to other methods, and the value of TS–YS also a maximum of 40 MPa.

In the case of method 'C', the low tensile strength was noted in the range 123–169 MPa for the trial C1–C3. Due to the dip-coating of pure aluminium on the AISI304L specimen (here, coated/buttered layer of 2 mm thick was acting as a barrier during FW), which may give the interference against the frictional effect between AISI304L and AA6063-T6 specimen during friction welding. As far as method 'C' is concerned, the welding parameters tried here were insufficient, and they would have to be raised to the higher values to obtain a sound weld joint with such a buttering layer on the specimen. The fine coating and the optimised welding parameters would be helpful to achieve the maximum strength by method C. Since the tensile strength of trial C1 was low to C2, the joining efficiencies were 60 % minimum and 82 % maximum. The easy fracture also happened next to the plastic zone with a 10.5 kN peak load for the C2 trial. The elongations (< 5 %) were poor due to the improper bonding between the welding materials. In this case, the welding pressures are to be much higher for getting good strength. Though the weld strength of the trials of method C was low compared to method 'A', it showed appreciable values of TS/YS ratio & TS–YS difference.

For method 'D', the joining needs some more friction time compared to method 'B' since much more effort needed to have the bonding between the inner groove and the outer of the taper on the specimens. All the trials in this method (D1–D3) showed good tensile and yield strength. Maximum tensile strength was 209.5 MPa with 191 MPa yield strength for the D3 trial. Anyhow, the yield point is the initial stage of starting the strain hardening region. The joint effi-

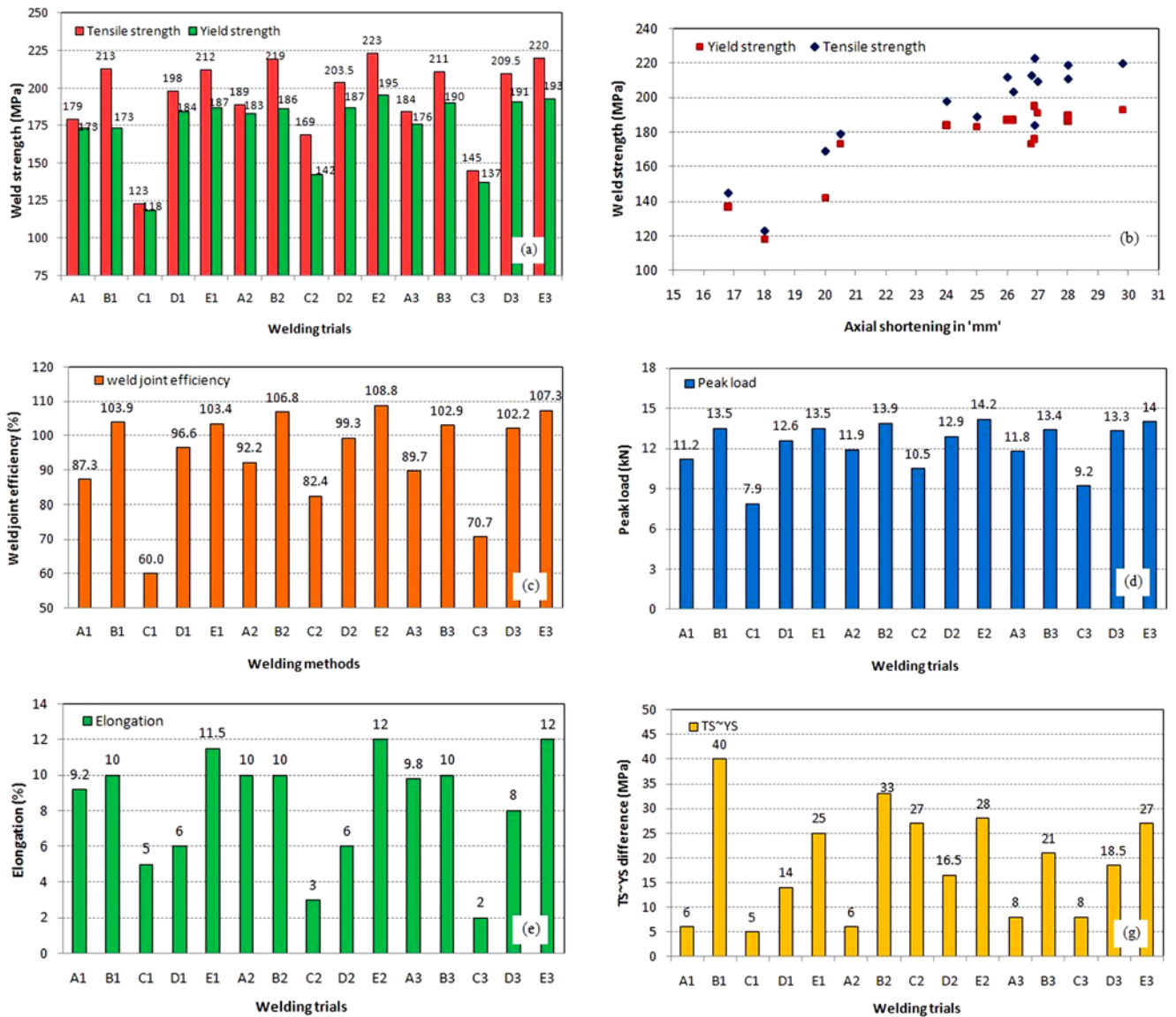


Fig. 8. Tensile testing results, where (a) tensile and yield strength, (b) relationship between axial shortening and weld strength, (c) weld efficiency, (d) peak load, (e) % elongation, (f) TS/YS ratio, and (g) TS–YS difference.

ciency was between 96–102%. For this method, weld joints observed a maximum peak load of 13 kN. The maximum elongation was 8% at a 7 s FT; it was a little less compared to the welding method ‘A’. This was because of the recess available on the AA6063-T6 specimen, which might reduce the elongation of the joint. If we study the tensile and yield strength relations, it is accepted that method ‘D’ produced a maximum of 1.1 TS/YS ratio and the TS–YS difference was 14–18 MPa.

The experiment with double tapering on both specimens, as mentioned in method ‘E’ in Fig. 2, showed fine results. The maximum yield and tensile strengths were obtained as 195 and 223 MPa, respectively, for the trial E2; these values are higher than those for the AA6063-T6 base alloy. Above 100% weld effi-

ciency was achieved for all the trials in the method ‘E’ like E1-E3. Thus the maximum tensile properties were achieved with the surface modifications. It had a maximum peak load of 14 kN, and the average axial shortening was about 27.5 mm that was the highest among the other welding methods. The elongation also reached the highest value of 12%, which is 2% higher than that of basic Al metal (8–10%). While observing the TS and YS relations, unlike other methods, the method ‘E’ showed an almost even strain hardening ratio around 1.13 or 1.14. Similarly, the TS–YS difference was also noted in the range 25–27 MPa, which may be low compared to method ‘B’.

The results show that the friction time and the welding methods are having effects on the tensile properties of dissimilar joints. No appreciable differences

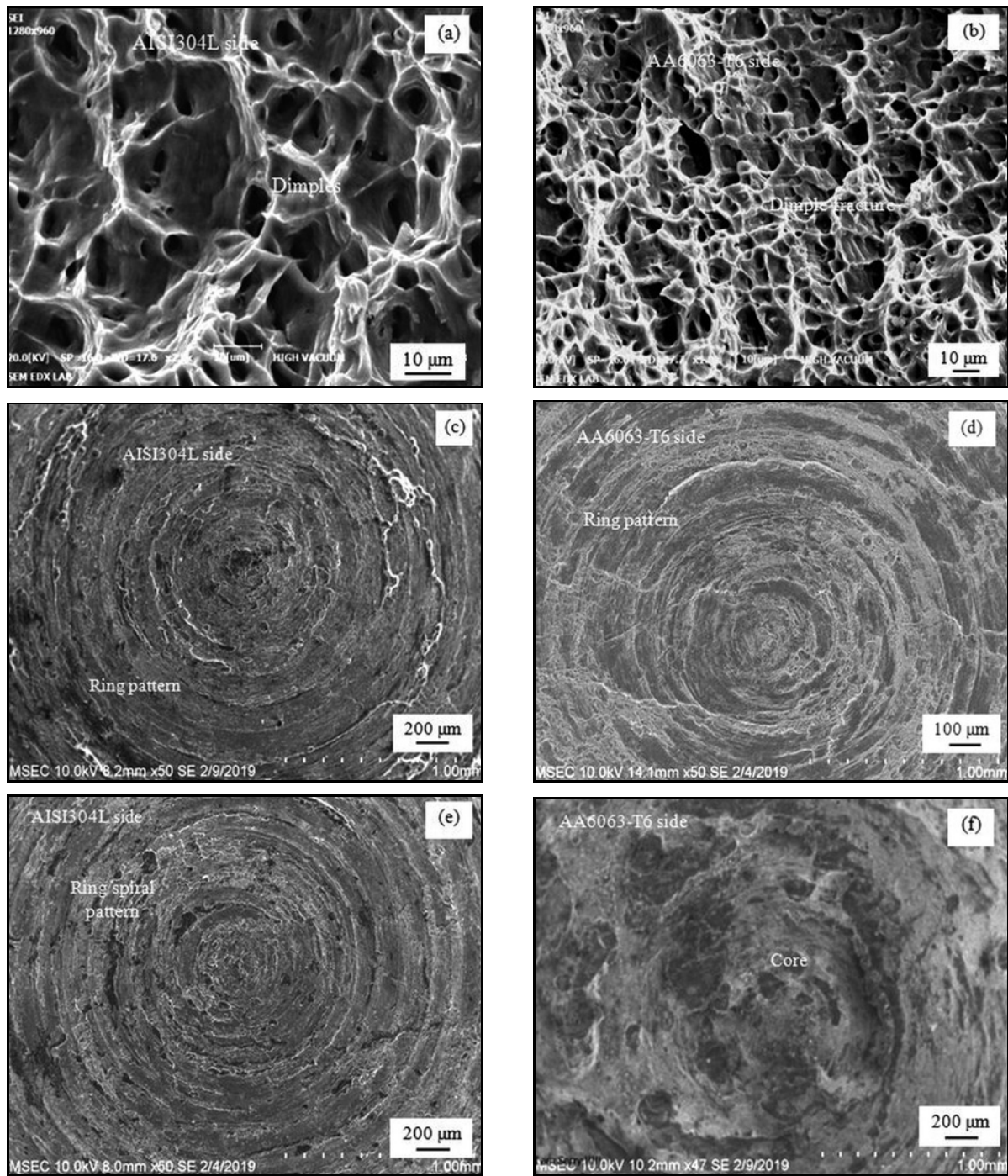


Fig. 9a–f. SEM images of the tensile fractured specimens, where (a), (b) – trial A2; (c), (d) – trial B2; (e), (f) – trial C2.

in the elongation values were observed for ‘E’ at different friction times. The maximum peak load was recorded for method ‘E’, whereas method ‘C’ had the required minimum load. During the experiment, it was observed that as the diameter of the weld specimen was small, the FT of 7 s was sometimes producing some weld defects like crack, maximum material loss and damaging the weld materials for this ferrous and non-ferrous combo.

It was hard to weld such small diameter speci-

mens with 7 s FT and at high FP. Thus it is suggested to identify the optimised parameters for the faying surface-modified welding process. The welding method ‘B’, ‘D’ shows good results at FT 3 s and these values further increased by increasing FT to 5 s. In most cases, 5 s FT showed better results except welding method ‘D’, which had appreciable results for 7 s FT. The joining efficiency had been improved by the faying surface modifications with the improvement in good bonding between metals.

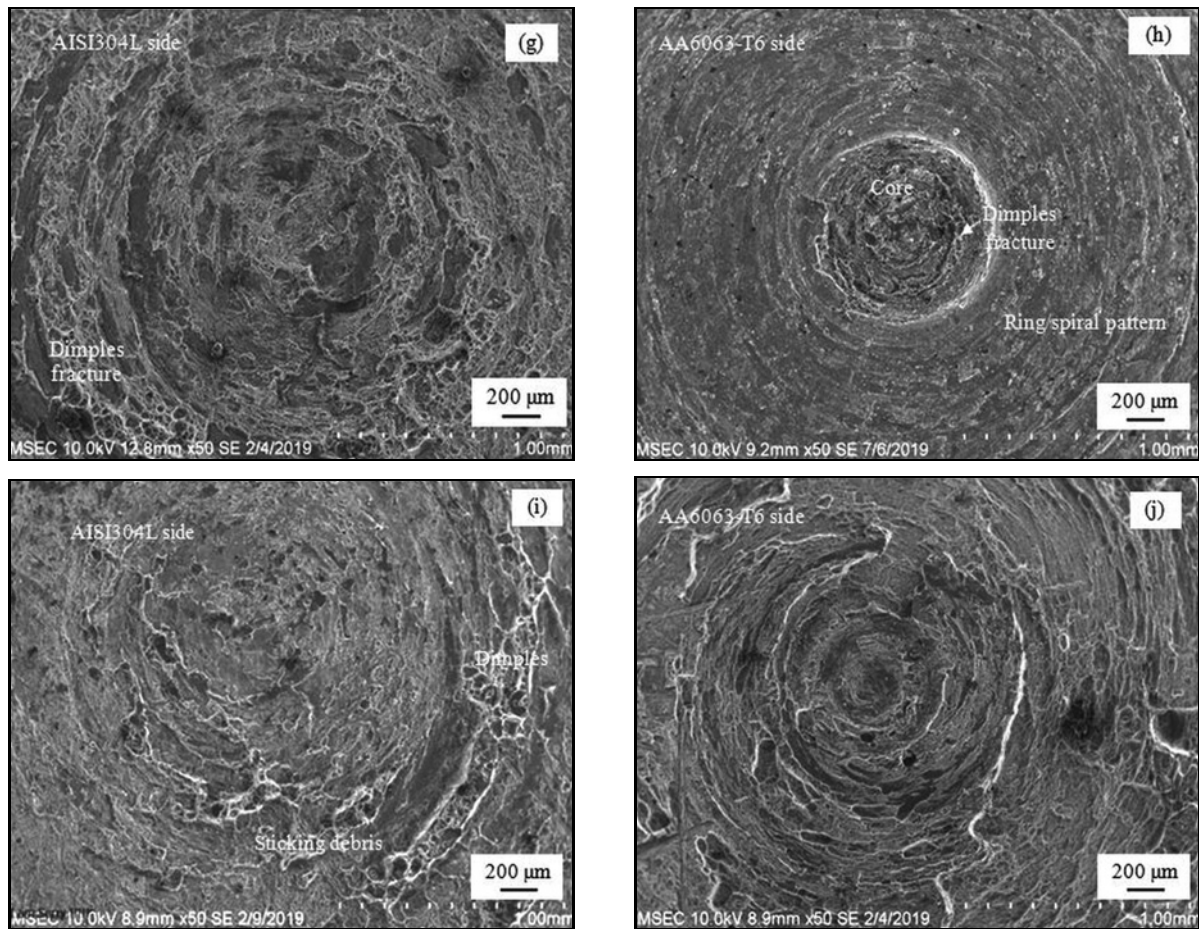


Fig. 9g–j. SEM images of the tensile fractured specimens, where (g), (h) – trial D3; (i), (j) – trial E2.

The ruptured specimens which had maximum tensile strength were analysed using SEM on both sides. Figures 9a–j show the SEM images of the tensile fractured specimens' parts. In the method 'A', trial A2 had maximum strength, and its fractography showed the dimple rupture on the AISI304L side and AA6063-T6 side. On the AA6063-T6 side, the dimples were closely packed and in minimum size compared to the AISI304L side. Trial A2 showed the ductile nature of the fractured specimen. Trial 'B2' also showed the formation of plastic deformation that happened during the tensile load. The spiral/ring pattern was found on both the AA6063-T6 and AISI304L sides, showing the frictional bonding during FW. In the SEM image, the AA6063-T6 debris is shown on both the AA6063-T6 and AISI304L sides.

For method C, the fracture analysis confirmed the brittle nature, which was mainly due to the incomplete bonding. Though the pure aluminium is soft, the welded parameters were insufficient in forming ductile structure, which led to the formation of brittle structure and non-effective bonding, which reduces the properties of the joints produced by trial 'C2'. The development of plastic deformation was shown in the

SEM image of trial 'D3'. The AA6063-T6 side had a small circle in its core which proved the neck formation. The SEM image of trial E2 is also seen in the figure. The dimple fracture is identified from that image, and the AA6063-T6 debris sticking on the AISI304L side is also shown.

The frictional effect on both the materials side was also visible. Thus the tried welding parameters created good bonding between the faying surfaces of both base metals. Through this fractography, the geometrical shape of the weld specimen was also one of the influences to develop the dimple structure of ductile nature. The friction pressure of 18 MPa was much enough for joining these AA6063-T6 and AISI304L of 12 mm diameter rods.

### 3.4. Charpy V-notch test and fracture analysis

The impact strength/toughness of the friction-welded dissimilar joints of AISI304L and AA6063-T6 was determined at room temperature, and the results are plotted in Fig. 10. Impact strength determines the energy absorbed by the welded joints in a cross-sectional area. Generally, Charpy impact was used to

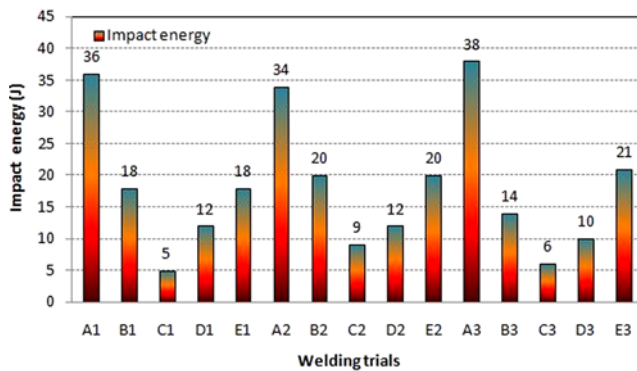


Fig. 10. Impact energy for the joints at different welding trials.

measure how easily a crack would initiate in a test specimen and how fast it would propagate once it was started [30]. The 'V' notch was positioned on the weld interface, as shown in Fig. 4b. According to Shanjeevi et al. [31], the temperature rise in the weld interface during friction welding and the alloying elements at

the weld interface may deteriorate the impact toughness of the welded joint. The faying surfaces of the materials to be joined by friction welding can show their effect on the performance of the welds manufactured [32].

The welding method 'A' had the weld specimens with the flat faying surface that showed better results than the others, and if the FT was increasing from 3 to 7 s, then the impact energy of the joint was also increasing. The maximum recorded impact was about 38 s for the 'A3' trial. The value recorded for the method 'B' was in the range of 14–20 J. Here the faying surfaces reduced the strength. FT 5 s showed better results, and the joining methods 'A' and 'E' were better than the others as far as impact energy was concerned. The impact strength obtained for the welding method 'C' was less than 9 J (trial C2). These values were much lesser than those of the other methods. The reason was that the incomplete bonding between metals happened due to the accumulation of pure liquid aluminium (by dipping) on the faying surface of AISI304L metal and the joint's brittle nature. All the trials under method D showed almost equal im-

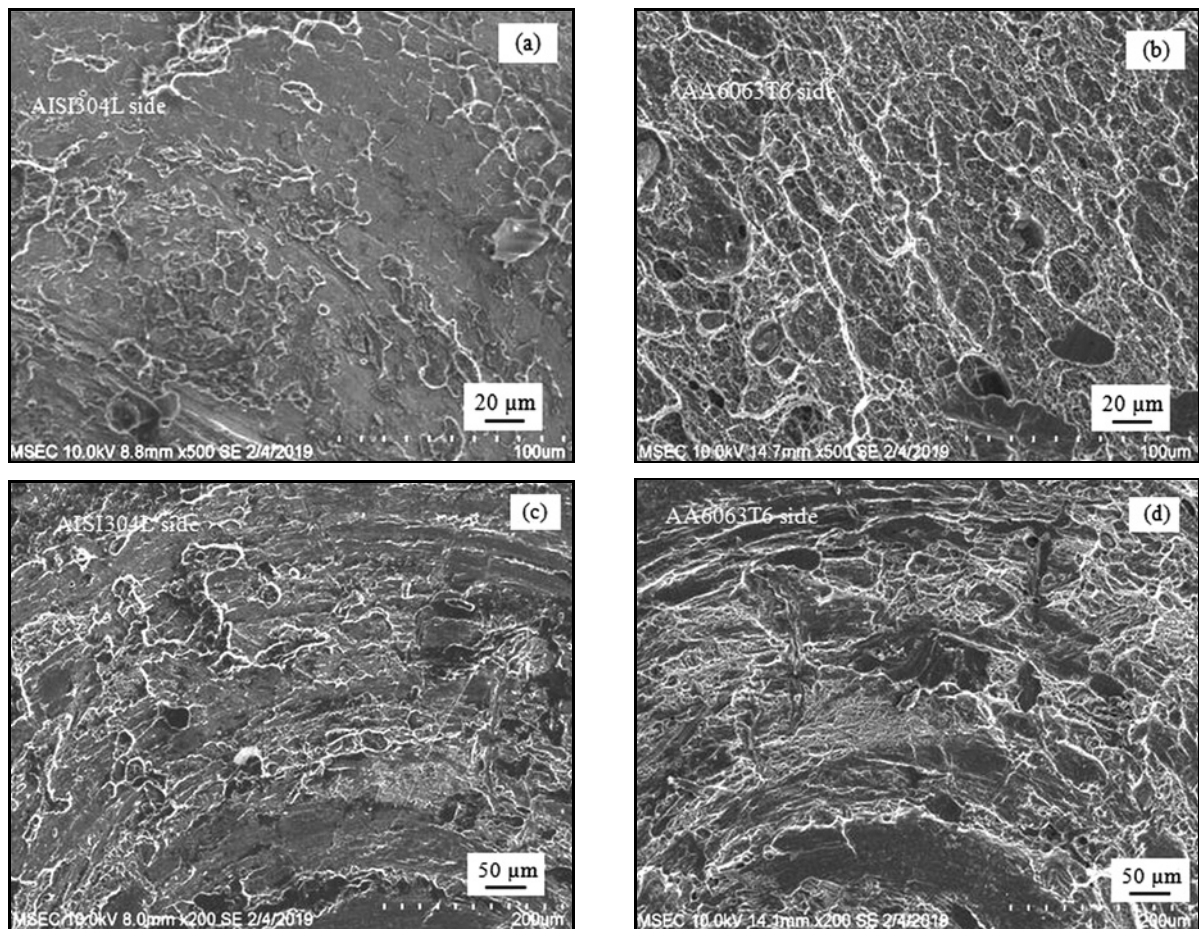


Fig. 11a–f. SEM images of fractured impact tested specimens, where (a), (b) – trial A3; (c), (d) – trial B2.

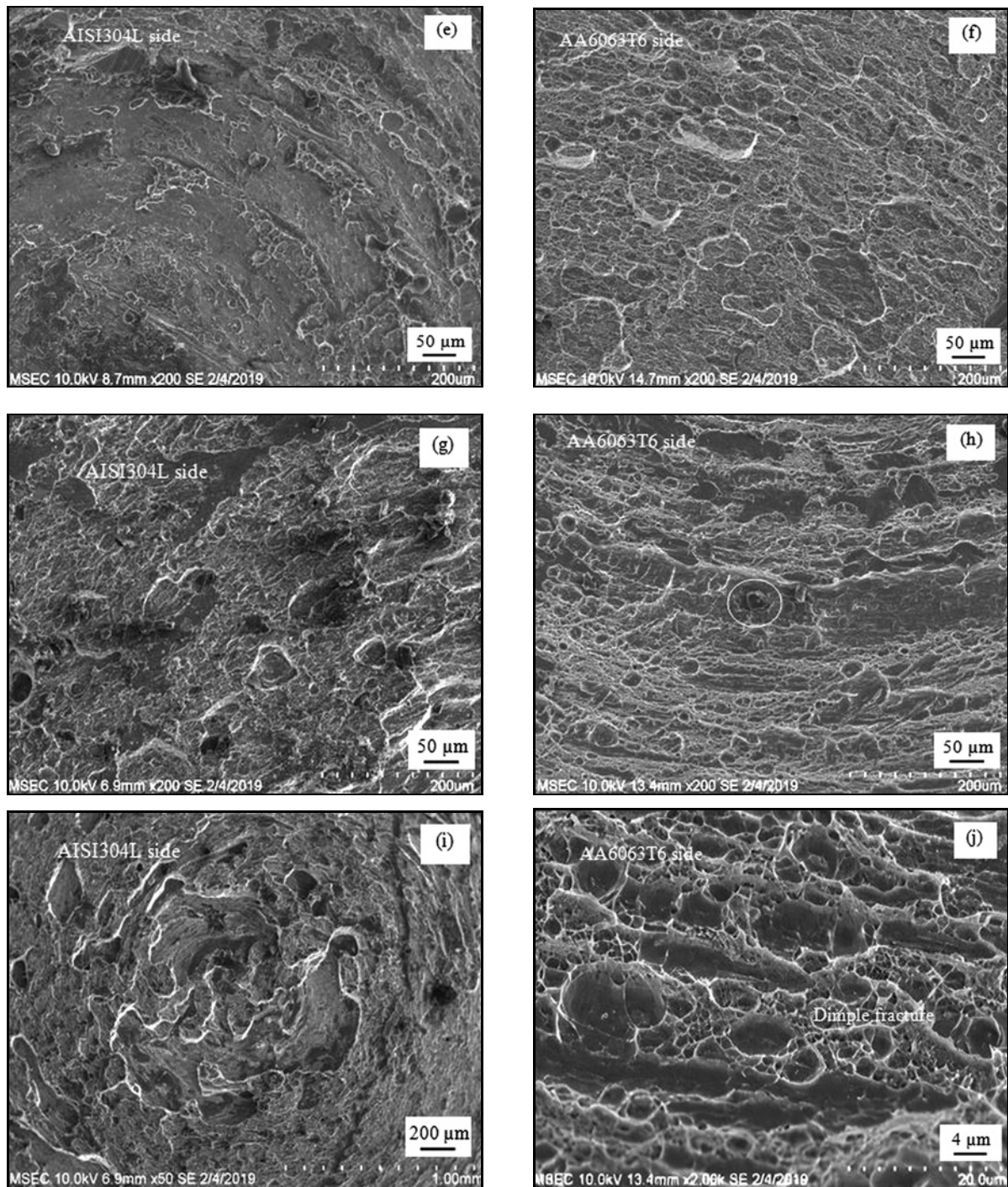


Fig. 11g–j. SEM images of fractured impact tested specimens, where (e), (f) – trial C2; (g), (h) – trial D1; (i), (j) – trial E3.

impact energy. But anyhow, the maximum of 14 J was recorded for 7 s FT. During experiments, it was difficult to weld with 18 MPa FP for 7 s FT. Method ‘E’ with tapering on both weld materials produced a maximum of 21 J impact energy. Since the huge pressure acted on the small diameter welding rods over a while, there was a possibility to cause damage to the AA6063-T6 material.

When analysing the impact tested specimens, the rupture was spotted on the V-notch position, and the fractures on both AISI304L and AA6063-T6 sides were analysed using SEM, and the images are shown in Fig. 11. The specimens which had maximum impact energy were analysed. Trial A2 shows the sliding in the AISI304L part and dimple with a congested layer on the AA6063-T6 side. For the B2 trial, the SEM

Table 4. Hardness distribution results along various regions of dissimilar joints

Experimental weld trials	AISI 304L side (HV 0.3)			AA6063-T6 side (HV 0.3)		
	Weld zone	HAZ	Base metal	Weld zone	HAZ	Base metal
A1	298	290	260	40	48	56
A2	288	274	269	48	49	78
A3	274	270	265	42	51	69
B1	323	312	303	68	72	80
B2	319	304	280	62	64	70
B3	315	307	303	69	71	75
C1	310	307	298	53	63	70
C2	315	309	303	59	62	72
C3	303	291	281	56	65	67
D1	320	314	308	55	70	77
D2	316	308	299	63	68	74
D3	312	305	296	56	68	70
E1	320	312	301	59	68	70
E2	317	310	303	58	70	76
E3	304	294	286	61	66	78

image shows the ductility nature of the joint while impact testing. But there was a difference in the rupture on the AA6063-T6 side of the A2 and B2 trials. The brittleness rupture is shown in the SEM images of trial C2. It meant that the impact strength was not high enough for the joint. Likely, trials D1 & E3 also made well-bonded joints, and they showed the dimple structure on both AA6063-T6 and AISI304L sides. The fractography varied according to the different faying surfaces. Thus the surface modifications and FT can influence the impact strength and the impact fracture of the joint manufactured through the rotary friction welding process.

### 3.5. Vickers microhardness analysis

The microhardness [33] distribution was measured using Vickers hardness tester along the welded zones from the weld interface to the base metals, and the observed values are given in Table 4. The Vickers microhardness distribution for all methods along with WI, HAZ, and the BM on both sides of the friction-welded dissimilar weld are plotted in Figs. 12a–e. The effects of FTs 3, 5, and 7 s were recorded for all the methods, and also the influence of faying surface modifications on the microhardness can be understood from the figures. The graphs were plotted concerning the hardness variation over a distance like 0.05, 3, and 1 mm from the weld interface line. The graphs show the hardness increasing from the weld interface of AA6063-T6 towards the BM of AA6063-T6. In contrast, hardness is decreasing from the weld interface to the AISI304L BM. Since the soft nature formed at the weld interface of the joint by method ‘A’, its hardness was less compared to others.

Method ‘B’ had good hardness values for 3 s FT,

and method ‘E’ was good for 5 s FT because of their tapering effect. The hardness of the welded zone was affected by friction pressure. Hardness nearby the weld interface on the AISI304L side increased as it had finer grains than the base zone. Comparing the hardness of all FTs, 3 s was responsible for maximum hardness. Thus the FT was influencing the hardness. As the FT increased, the temperature production and the intermetallic formation at the weld interface further grew. Due to this, there may be a decrease in hardness values for 7 s FT compared to 3 s FT. The hardness increases near the weld bonding area as the metals experienced massive plastic deformation due to the frictional force. From the figures, it is understood that the faying surface modifications may vary the hardness of the joints, too.

The microhardness of how it differs along with the distances from the weld interface to the base metals on both the AA6063-T6 and AISI304 sides according to the friction time variations and the joining methods can be seen in Fig. 12. For the sake of the reader’s convenience, the microhardness of the AISI304L and AA6063-T6 sides results for all the FTs 3, 5, and 7 s are combined in one graph and individually analysed for each method. The hardness decreases with the increase of aluminium content in the weld zone.

## 4. Conclusions

In this study, AA6063-T6 alloy was successfully welded with AISI304L steel through the rotary friction welding process with different faying surface modifications at different welding trials. New surface modifications on weld specimens were tried in this study, and their effects on mechanical properties, microstruc-

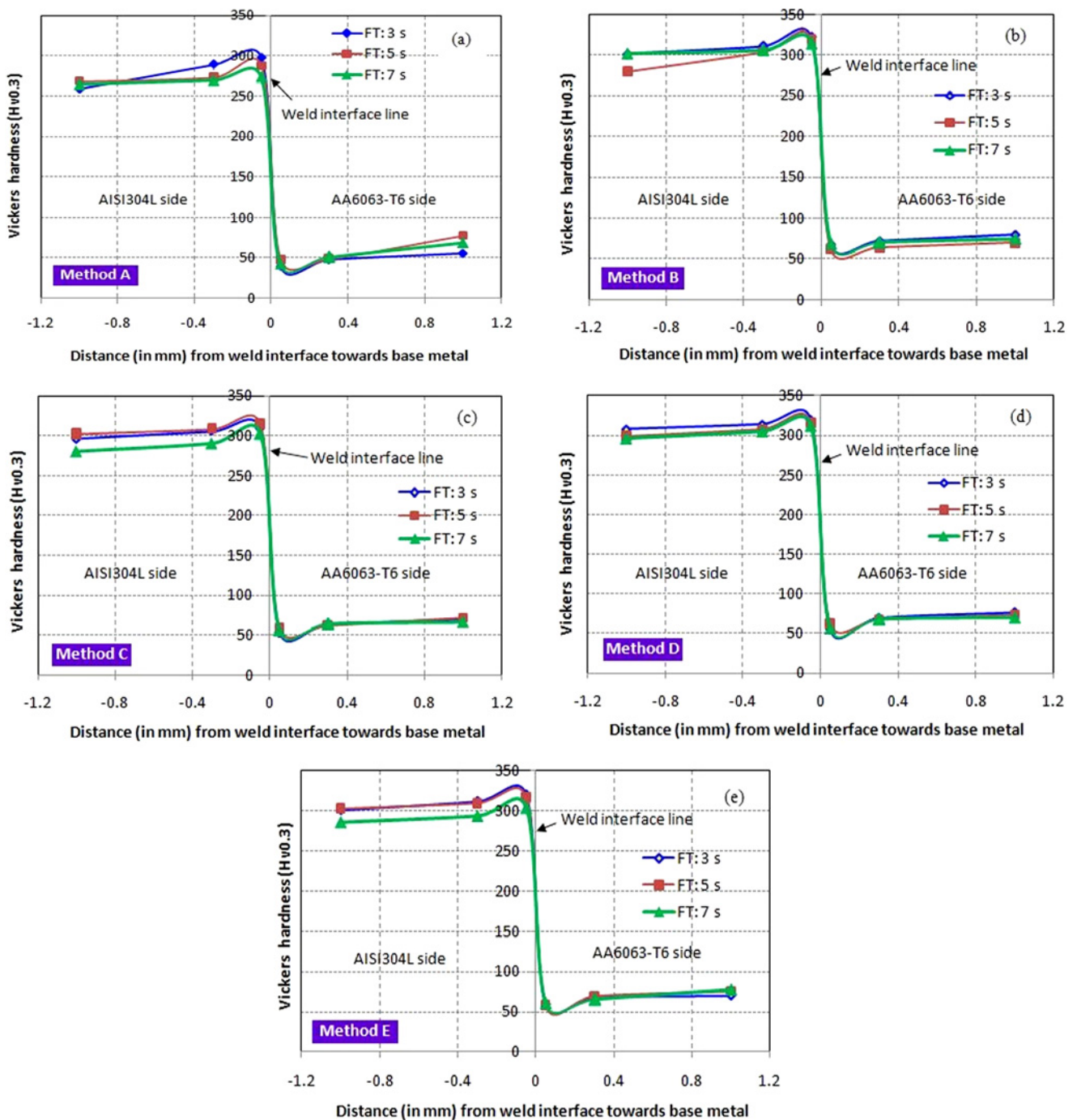


Fig. 12. Vickers microhardness distribution along the weld zone for all joining methods (A to E) & FTs, where (a) method A, (b) method B, (c) method C, (d) method D, and (e) method E.

tures, and fractography were analysed, and the conclusions are reported. All the faying surface modifications (method A to E) were favourable for the weld materials. EDS spectrum showed the formation of Fe-Al intermetallics on WI, and microstructure proved the good bonding between the metals with the narrow HAZ. Method 'B' produced 'V' shaped WI. FT showed its effects on the joint properties, and 5 s FT produced better results. During FW, 7 s FT can have

the possibility to damage the  $\phi$  12 mm small diameter metals at high FP. The faying surfaces increased the bonding between metals and improved tensile strength. The maximum tensile strength obtained was 223 MPa with 195 MPa yield strength for the trial E2. During testing, all the breakages happened outside the weld joint except for welding method 'C'. The elongation was observed up to 12%, which is higher than standard AA6063-T6 base metal. Joining methods B,

D, and E produced almost 100 % joint efficiency.

The tensile rupture images showed trans-granular dimple fracture except for trial 'C2', which showed intergranular brittleness. The method 'A' with flat faying surfaces showed good impact toughness with a maximum of 38 J, and the tapered faying surface reduced the impact energy. The hardness increased near the weld bonding area of the AISI304L side as the metals experienced massive plastic deformation due to friction. But, the hardness was increasing from WI to base metal of AA6063-T6 side. The elongated grains were found nearby WI. The hardness of AISI304L WI was around  $\geq 300 \text{ HV}_{0.3}$ , which was in the range of 40–69  $\text{HV}_{0.3}$  for AA6063-T6 WI.

### References

- [1] P. K. Baghel, D. S. Nagesh, Mechanical properties and microstructural characterisation of automated pulse TIG welding of dissimilar aluminium alloy, *Indian Journal of Engineering & Materials Sciences* 25 (2018) 147–154.
- [2] N. Srirangarajulu, A. Rajadurai, Hardness and tensile behaviour of friction stir welded Cu-40wt.%Zn brass, *Indian Journal of Engineering & Materials Sciences* 24 (2017) 63–68. <http://nopr.niscair.res.in/handle/123456789/42620>
- [3] J. Lesniewski, A. Ambroziak, Modelling the friction welding of titanium and tungsten pseudoalloy, *Archives of Civil and Mechanical Engineering* 15 (2015) 142–150. [doi:10.1016/j.acme.2014.06.008](https://doi.org/10.1016/j.acme.2014.06.008)
- [4] P. Sathiya, S. Aravindan, A. Noorul Haq, Effect of friction welding parameters on mechanical and metallurgical properties of ferritic stainless steel, *Int. Journal of Advanced Manufacturing Technology* 31(2007) 1076–1082. [doi:10.1007/S00170-005-0285-5](https://doi.org/10.1007/S00170-005-0285-5)
- [5] M. Kessler, S. Suenger, M. Haubold, M. F. Zaeh, Modelling of upset and torsional moment during inertia friction welding, *Journal of Materials Processing Technology* 227 (2016) 34–40. [doi:10.1016/j.jmatprotech.2015.07.024](https://doi.org/10.1016/j.jmatprotech.2015.07.024)
- [6] L. Fratini, G. Buffa, M. Cammalleri, D. Campanella, On the linear friction welding process of aluminium alloys: Experimental insights through process monitoring, *CIRP Annals-Manufacturing Technology* 62 (2013) 295–298. [doi:10.1016/j.cirp.2013.03.056](https://doi.org/10.1016/j.cirp.2013.03.056)
- [7] O. Iracheta, C. J. Bennett, W. A. Sun, Sensitivity study of parameters affecting residual stress predictions in finite element modelling of the inertia friction welding process, *International Journal of Solids and Structures* 71 (2015) 180–193. [doi:10.1016/j.ijsolstr.2015.06.018](https://doi.org/10.1016/j.ijsolstr.2015.06.018)
- [8] M. Kimura, K. Suzuki, M. Kusaka, K. Kaizu, Effect of friction welding condition on joining phenomena, tensile strength, and bend ductility of friction welded joint between pure aluminium and SS304 stainless steel, *Journal of Manufacturing Processes* 25 (2017) 116–125. [doi:10.1016/j.jmapro.2016.12.001](https://doi.org/10.1016/j.jmapro.2016.12.001)
- [9] C. Liu, C.-L. Dong, Internal residual stress measurement on linear friction welding of titanium alloy plates with contour method, *Trans. Nonferrous Met. Soc. China* 24 (2014) 1387–1392. [doi:10.1016/s1003-6326\(14\)63203-9](https://doi.org/10.1016/s1003-6326(14)63203-9)
- [10] M. Meisnar, S. Baker, J. M. Bennett, A. Bernad, A. Mostafa, S. Resch, N. Fernandes, A. Norman, Microstructural characterisation of rotary friction welded AA6082 and Ti-6Al-4V dissimilar joints, *Materials and Design* 132 (2017) 188–197. [doi:10.1016/j.matdes.2017.07.004](https://doi.org/10.1016/j.matdes.2017.07.004)
- [11] G. Buffa, M. Cammalleri, D. Campanella, L. Fratini, Shear coefficient determination in linear friction welding of aluminium alloys, *Materials and Design* 82 (2015) 238–246. [doi:10.1016/j.matdes.2015.05.070](https://doi.org/10.1016/j.matdes.2015.05.070)
- [12] J. Akram, P. Rao Kalvala, M. Misra, I. Charit, Creep behaviour of dissimilar metal joints between P91 and SS304, *Materials Science and Engineering A* 688 (2017) 396–406. [doi:10.1016/j.msea.2017.02.026](https://doi.org/10.1016/j.msea.2017.02.026)
- [13] L. Donati, E. Troiani, P. Proli, L. Tomesani, FEM analysis and experimental validation of friction welding process of 6xxx alloys for the prediction of welding quality, *Materials Today: Proceedings* 2 (2015) 5045–5054. [doi:10.1016/j.matpr.2015.10.095](https://doi.org/10.1016/j.matpr.2015.10.095)
- [14] S. Nandy, K. Kumar Ray, D. Das, Process model to predict yield strength of AA6063 alloy, *Materials Science and Engineering A* 644 (2015) 413–424. [doi:10.1016/j.msea.2015.07.070](https://doi.org/10.1016/j.msea.2015.07.070)
- [15] T. Watanabe, H. Takayama, A. Yanagisawa, Joining of aluminum alloy to steel by friction stir welding, *Journal of Materials Processing Technology* 178 (2006) 342–349. [doi:10.1016/j.jmatprotec.2006.04.117](https://doi.org/10.1016/j.jmatprotec.2006.04.117)
- [16] H.-S. Bang, H.-S. Bang, K.-H. Kim, Effects of process parameters on friction stir weldability in dissimilar joints of AA5052 and advanced high strength steel, *Journal of Welding and Joining* 39 (2021) 189–197. [doi:10.5781/JWJ.2021.39.2.8](https://doi.org/10.5781/JWJ.2021.39.2.8)
- [17] E. Taban, J. E. Gould, J. C. Lippold, Dissimilar friction welding of 6061-T6 aluminum and AISI 1018 steel: Properties and microstructural characterisation, *Materials & Design* (1980–2015) 31 (2010) 2305–2311. [doi:10.1016/j.matdes.2009.12.010](https://doi.org/10.1016/j.matdes.2009.12.010)
- [18] S. D. Meshram, G. Madhusudhan Reddy, Friction welding of AA6061 to AISI 4340 using silver interlayer, *Defence Technology* 11 (2015) 292–298. [doi:10.1016/j.dt.2015.05.007](https://doi.org/10.1016/j.dt.2015.05.007)
- [19] P. Kannan, K. Balamurugan, K. Thirunavukkarasu, Influence of silver interlayer in dissimilar 6061-T6 aluminum MMC and SS304L stainless steel friction welds, *The International Journal of Advanced Manufacturing Technology* 81 (2015) 1743–1756. [doi:10.1007/s00170-015-7288-7](https://doi.org/10.1007/s00170-015-7288-7)
- [20] C. H. Muralimohan, M. Ashfaq, R. Ashiri, V. Muthupandi, K. Sivaprasad, Analysis and characterisation of the role of Ni interlayer in the friction welding of titanium and 304 austenitic stainless steel, *Metall. Mater. Trans. A* 47 (2016) 347–359. [doi:10.1007/s11661-015-3210-z](https://doi.org/10.1007/s11661-015-3210-z)
- [21] J. R. Davis, *Aluminum and Aluminum Alloys*. ASM International, Materials Park, 2001. [doi:10.1361/autb2001p351.OLD15](https://doi.org/10.1361/autb2001p351.OLD15)
- [22] S. O. Adeosun, E. I. Akpan, O. I. Sekunowo, W. A. Ayoola, S. A. Balogun, Mechanical characteristics of 6063 aluminum steel dust composite, *International Scholarly Research Notices* 2012 (2012) 461853. [doi:10.5402/2012/461853](https://doi.org/10.5402/2012/461853)

- [23] G. M. Karthik, P. Mastanaiah, G. D. Janaki Ram, R. S. Kottada, Friction buttering: A new technique for dissimilar welding, *Metallurgical and Materials Transactions B* 48 (2017) 1416–1422. [doi:10.1007/s11663-017-0934-8](https://doi.org/10.1007/s11663-017-0934-8)
- [24] C. Leitao, E. Arruti, E. Aldanondo, D. M. Rodrigues, aluminium-steel lap joining by multi pass friction stir welding, *Materials and Design* 106 (2016) 153–160. [doi:10.1016/j.matdes.2016.05.101](https://doi.org/10.1016/j.matdes.2016.05.101)
- [25] M. Kimura, A. Fuji, S. Shibata, Joint properties of friction welded joint between pure magnesium and pure aluminium with post-weld heat treatment, *Materials and Design* 85 (2015) 169–179. <http://dx.doi.org/10.1016/j.matdes.2015.06.175>
- [26] M. Deepak, D. Ananthapadmanaban, Welding mechanisms during friction welding of aluminium with steel, *Journal of Chemical and Pharmaceutical Sciences* 7 (2017) 53–55.
- [27] M. Mohammed Asif, S. Kulkarni Anup, P. Sathiya, Finite element modelling and characterisation of friction welding on UNS S31803 duplex stainless steel joints, *Engineering Science and Technology, an International Journal* 18 (2015) 704–712. [doi:10.1016/j.jestch.2015.05.002](https://doi.org/10.1016/j.jestch.2015.05.002)
- [28] P. M. Ajith, T. M. Afsal Husain, P. Sathiya, S. Aravindan, Multi-objective optimisation of continuous drive friction welding process parameters using response surface methodology with intelligent optimisation algorithm, *Journal of Iron and Steel Research International* 22 (2015) 954–960. [doi:10.1016/S1006-706X\(15\)30096-0](https://doi.org/10.1016/S1006-706X(15)30096-0)
- [29] P. Zhang, S. X. Li, Z. F. Zhang, General relationship between strength and hardness, *Materials Science and Engineering A* 529 (2011) 62–73. [doi:10.1016/j.msea.2011.08.061](https://doi.org/10.1016/j.msea.2011.08.061)
- [30] S. Senthil Murugan, A. Noorul Haq, P. Sathiya, Eco-friendly frictional joining of AA6063 and AISI304L dissimilar metals and characterisation of bimetal joints, *Journal of New Materials for Electrochemical Systems* 23 (2020) 101–111. [doi:10.14447/jnmes.v23i2.a07](https://doi.org/10.14447/jnmes.v23i2.a07)
- [31] C. Shanjeevi, J. Jeswin Arputhabalan, R. Dutta, Pradeep, Investigation on the effect of friction welding parameters on impact strength in dissimilar joints, *IOP Conf. Series: Material Science and Engineering* 197 (2017) 012069. [doi:10.1088/1757-899X/197/1/012069](https://doi.org/10.1088/1757-899X/197/1/012069)
- [32] M. Senthil, S. P. Sathiya, N. Haq, An experimental study on the effect of silver, nickel and chromium interlayers and upset pressure in joining SS304L-AA6063 alloys through direct drive friction welding process, *J. Braz. Soc. Mech. Sci. Eng.* 42 (2020) 611. [doi:10.1007/s40430-020-02687-7](https://doi.org/10.1007/s40430-020-02687-7)
- [33] A. Klimová, J. Lapin, Effect of Al content on microstructure of Ti-Al-Nb-C-Mo composites reinforced with carbide particles, *Kovove Mater.* 57 (2019) 377–387. [doi:10.4149/km\\_2019\\_6\\_377](https://doi.org/10.4149/km_2019_6_377)